Multiple Beam Atomic Interferometer

M. Weitz, T. Heupel, and T. W. Hänsch

Max-Planck-Institut für Quantenoptik, 85748 Garching, Germany
(Received 4 December 1995)

We have demonstrated a multiple beam atom interferometer. Atoms in a cesium atomic beam are optically pumped into a spatially separating nonabsorbing superposition state consisting of five partial beams in different Zeeman sublevels separated by a momentum of two photon recoils each. When the partial waves are spatially recombined, we observe an interference signal which shows the sharply peaked Airy pattern characteristic for multiple beam interference.   [S0031-9007(96)01220-3]

PACS numbers: 03.75.Dg, 07.60.Ly, 32.80.Lg, 42.50.Vk

In recent years several groups have demonstrated two-beam interferometers with neutral atoms [1]. Atom interferometers have now been used to measure the acceleration due to gravity, rotations, and the photon recoil of an atom [1–3].

In this Letter we describe an atom interferometer with multiple paths. Whereas all previously realized atom interferometers have observed sinusoidal fringes resulting from two-beam interference, we measure a fringe pattern that resembles the sharply peaked Airy function known, e.g., from an optical Fabry-Pérot interferometer [4]. The sharper fringes translate to a higher resolution compared to that of the corresponding two-beam atom interferometer.

In our experiment, we use a cesium atomic beam and two counterpropagating optical beams in a $\sigma^+ - \sigma^-$ polarization configuration resonant with the cesium $D1$ line. In a first laser pulse, atoms are optically pumped into a nonabsorbing "dark" coherent superposition of five magnetic ground state Zeeman sublevels separated by a momentum of two photon recoils each (Fig. 1). For this coherent superposition of states, the absorption amplitudes into the excited levels initially precisely cancel. The wave packets are allowed to spatially separate for a time T, after which a second pulse is applied. Since the wave packets have spatially separated, the atom cannot be in a completely dark state for the light field by the time of the second pulse. The second pulse splits each of the wave packets into five further wave packets. Finally, a third pulse at time T after the second pulse recombines the trajectories to several families of interfering wave packets. To read out the interferometer, we detect the fluorescence emitted during the final pulse as a function of the phase of this pulse. With no additional phase, the atoms are already again in a dark state at this time and no fluorescence is emitted. When the phase is varied, fluorescence can be observed since the atoms are not dark any more for the light field. The fluorescence vanishes only when the phase difference between adjacent paths is close to an integer multiple of 2π. The dips in fluorescence observed when the phase is varied become increasingly sharp with a larger number of paths. We

demonstrate here that such an interferometer can be realized experimentally quite easily.

It has been proposed to use adiabatic passage through a dark superposition state for atomic beam splitters [5]. Momentum transfer with this technique was later demonstrated [6]. An atomic two-beam interferometer based on a dark state in a three-level system is described in Ref. [7], where the population and momentum was transferred between two ground state levels by adiabatic passage and the geometry of a 4 $\pi/2$ pulse interferometer [8] was used. Here we use a "dark state" analog of the simpler $\pi/2$-π-$\pi/2$ pulse interferometer [2] with a pulse
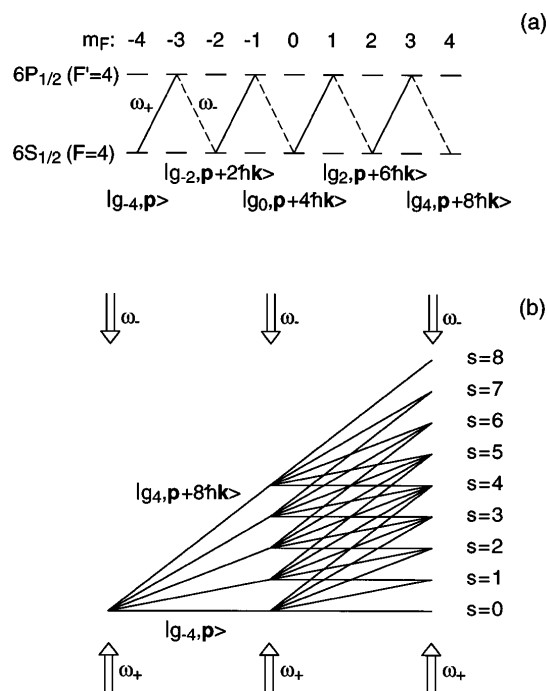

FIG. 1. (a) Level scheme for a velocity dependent dark state in a chain of four Λ transitions using the transition $6S_{1/2}(F = 4)$-$6P_{1/2}(F' = 4)$ of the cesium $D1$ line. (b) Scheme of an atomic multiple beam interferometer. The contributions of the different families of interfering wave packets (numbered $s = 0, \ldots, 8$) to the total signal are shown in Fig. 2 (left).

scheme known from NMR spin echo experiments [9]. Our method, based on three successive optical pumping pulses, is applicable both to three-level and multilevel systems.

A multiple beam atom interferometer with N paths can be realized with a transition from a ground state of total angular momentum $F = N - 1$ to an excited state with a total angular momentum F'. For $F' = F$ one dark state exists, and the atom is pumped into a coherent superposition of N magnetic ground state sublevels, where each m_F sublevel is associated with a distinct momentum. It can be shown that at time t after a pumping pulse the dark state has evolved into the coherent superposition

$$|\varphi_D(t)\rangle = \sum_{n=0}^{N-1} w_n e^{-it\delta_n} |g_{2n-N+1}, \mathbf{p} + n\hbar(\mathbf{k}_+ - \mathbf{k}_-)\rangle,$$

(1)

where $|g_{m_F}, \mathbf{p}\rangle$ denotes a ground state of magnetic quantum number m_F and momentum $\mathbf{p}$, and $\mathbf{k}_{\pm}$ are the wave vectors of the σ^+ and σ^- polarized waves. The weights w_n are determined by the Clebsch-Gordan coefficients and are such that $|\varphi_D(t = 0)\rangle$ is a dark state for the light field. Here we assume that the electric field amplitudes for both polarizations are equal at all times. The Raman detunings δ_n are

$$\delta_n = n[\Delta\omega - (\mathbf{k}_+ - \mathbf{k}_-) \cdot \mathbf{p}/m] - n^2\omega_r, \quad (2)$$

where $\Delta\omega = \omega_+ - \omega_- - \omega_A$ with $\omega_{\pm} = c|\mathbf{k}_{\pm}|$; ω_A denotes the splitting between two adjacent even m_F levels, and $\omega_r = \hbar(\mathbf{k}_+ - \mathbf{k}_-)^2/2m$ the recoil energy of a single Raman transition in frequency units. Note that if $\mathbf{k}_+ \neq \mathbf{k}_-$ the dark state is never completely stationary for such a chain of Raman transitions, since the recoil term quadratic in n prevents the simultaneous tuning of all δ_n to zero for $N > 2$ [10]. We circumvent this leakage by keeping the lengths of the pumping pulses short, so that the frequency width of the dark state [11] is larger than the recoil energy of eight photons (≈ 120 kHz).

The expected interferometer signal is calculated as follows. We assume that the first pumping pulse ends at time $t = 0$ and leaves the atom in the coherent superposition given by Eq. (1) with all exponential equal to unity. At the time $t = T$ when the second pulse is applied, the atom is in general in a superposition of the dark state and the coupled states. The second pulse will remove most of the population that is not in the dark state. After a few fluorescent cycles these atoms will be pumped to the $F = 3$ ground state and not be detected any more. The part that remains in the dark state is given by the projection

$$\langle \varphi_D(T) | \varphi_D(0) \rangle = \sum_{n=0}^{N-1} w_n^2 e^{i\delta_n T}, \quad (3)$$

where we have neglected the fraction of atoms that are repumped into the dark state by the second pulse, resulting in a background to the fringe pattern.

Formula (3) already gives the interference signal for a Ramsey type experiment with only two laser pulses and

copropagating beams ($\mathbf{k}_+ = \mathbf{k}_-$). The detunings here are $\delta_n = n\Delta\omega$, which is linear in n. If all weights w_n were equal, one easily derives that the probability for the atom to be in the dark state after the second pulse would be proportional to $\sin^2(N\Delta\omega T/2)/\sin^2(\Delta\omega T/2)$. This expression is identical to the well-known diffraction pattern of a grating with N slits [4]. The unequal Clebsch-Gordan coefficients for an atom—corresponding to a grating with different transmissions of the individual "slits"—will now lower the principal maxima and increase the side maxima.

For counterpropagating laser beams (we assume $\mathbf{k}_+ = k\mathbf{e}_z$, $\mathbf{k}_- = -k\mathbf{e}_z$) the atomic wave packets will spatially separate after the first pulse. In a momentum basis picture, the initial momentum spread $f(v_z)$ associated with the finite size of the atomic wave packet will introduce different Doppler dephasings for the atoms [see Eq. (2)]. The second pulse now again projects the atom onto the dark state. Each of the spatially separated components can be decomposed into the dark state and several coupled states. The coupled state amplitudes are filtered by the second pulse, and what remains is the splitting of each initial path into five further paths. Interference can be observed with a third pulse, where several atomic wave packets spatially recombine. We now assume that the phase of the light with frequency ω_+ is varied by $\delta\theta$ for the third pulse. This is equivalent to a small variation of the Raman detuning between the second and third pulse. After summing all the momentum states and including a second factor, as in Eq. (3), for the second projection, we obtain the following wave function after the final pulse

$$|\Psi(t)\rangle = \int f(p_z) |\varphi_D(t), p_z\rangle \sum_{n=0}^{N-1} \sum_{q=0}^{N-1} w_n^2 w_q^2$$
$$\times \exp\{i[(n + q)(\Delta\omega - 2kp_z/m)T$$
$$+ q\delta\theta - (n^2 - q^2)\omega_r T]\} dp_z. \quad (4)$$

In the expression for the probability $\||\Psi\rangle|^2$ of an atom to remain in the dark state after the final pulse, we can solve the integral for an atomic velocity distribution sufficiently broad ($2k\Delta v_z T \gg 2\pi$) and smooth. Using now $s = n + q$, the resulting expression can be written as

$$\||\Psi\rangle|^2 = \sum_{s=0}^{2N-2} \||\Psi_s\rangle|^2, \quad (5)$$

where

$$|\Psi_s\rangle = \sum_q w_{s-q}^2 w_q^2 \exp\{i[q\delta\theta + (sq - q^2)2\omega_r T]\}.$$

(6)

The sum over q runs from $\max(0, s - N + 1)$ to $\min(N - 1, s)$. The obtained signal is independent of $\Delta\omega$. This insensitivity to the frequency detuning is known for a spin echo experiment. The wave function $|\Psi_s\rangle$ describes the interference of a family with $N - (|s - N + 1|)$ beams that spatially recombine during the

final pulse, as shown in Fig. 1(b). For $\omega_r T \rightarrow 0$, when the recoil term in Eq. (6) can be neglected, all these families of interfering wave packets have their principal maxima at phases $\delta\theta$ of integer multiples of 2π. The contributions of the different families to the total signal in this limit are shown in Fig. 2 (left) for $N = 5$. The family with five paths and $s = 4$ has the sharpest principal maxima, and also gives the largest contribution to the total signal. We obtain Airy type fringes similar to the Doppler-free, two-pulse arrangement.

Figure 2 (right) shows some theoretical interference fringe patterns for different interaction times T. For larger times T, the recoil term significantly affects the relative intensities of the individual maxima and destroys the Airy type pattern. However, when the interaction time T is an integer multiple of π/ω_r (≈ 66.8 μs here), Eq. (6) shows that the original fringe pattern is revived. These phenomena are usually not observed in a two-beam geometry and are an interesting feature of multiple beam interferometers. For practical applications in most cases it will be reasonable to set the interaction time T precisely to a revival time, which gives the maximum fringe contrast.

In our experiment an effusive cesium atomic beam is emitted by an oven through a 200 μm wide slit into a vacuum chamber with a pressure of 10^{-6} Torr. A 250 μm wide second slit located 25 cm away collimates the beam in a direction longitudinal to the optical beams, before the atoms enter the laser interaction region. Three orthogonal pairs of Helmholtz coils create a magnetic bias field of 300 mG along the optical beams and null transverse magnetic fields. A photomultiplier and a boxcar integrator record the fluorescence emitted during the pulses.

The two optical beams are generated by a Ti:sapphire laser whose frequency is locked to the $6S_{1/2}(F = 4)$-$6P_{1/2}(F' = 4)$ transition near 894 nm. A first acousto-optic modulator generates the pulse shapes for the optical beams. The light is then split up into two beams, each of which passes a further acousto-optic modulator which shifts their optical frequencies by slightly different amounts in order to maintain the two-photon resonance condition ($\Delta\omega = 0$) in the presence of the bias field. The phase of the drive frequency of one of these frequency shifters can be changed during the pulse sequence to allow the adjustment of the phase of one of the optical beams in the final pulse. The two pumping beams are spatially filtered and expanded to a diameter of 3 cm. The typical optimum power in each beam is 150 mW, corresponding to a Rabi frequency of ≈ 4 natural widths for the weakest transitions in the beam center. All the interferometer pulses are applied during the transit time of the atoms through the optical interaction region.

The repetition rate of a typical interferometer pulse sequence is 8 kHz. We alternate between a pulse sequence with the phase of the beam with frequency ω_+ shifted at the final pulse and a sequence with no extra phase shift. By recording the difference of the two obtained fluorescence signals with a lock-in amplifier, we can suppress the effect of stray light.

Typical Ramsey signals obtained with two resonant optical pulses (width 0.7 μs) separated by a time $T = 5$ μs are shown in Fig. 3. The pumping pulses here were provided with copropagating beams. The observed full width of the principal maxima is $0.21 \times 2\pi$, which is slightly broader than the theoretically expected value of $0.16 \times 2\pi$. We believe that this, as well as the slight asymmetry in the heights of the side maxima, is due to inhomogeneous stray magnetic fields. A possible application of this dark state Ramsey experiment is the use as a sensitive method for detection of magnetic fields. Magnetic coherences of unpolarized atoms have previously been observed in the contrast of a two-beam atom interferometer [12].
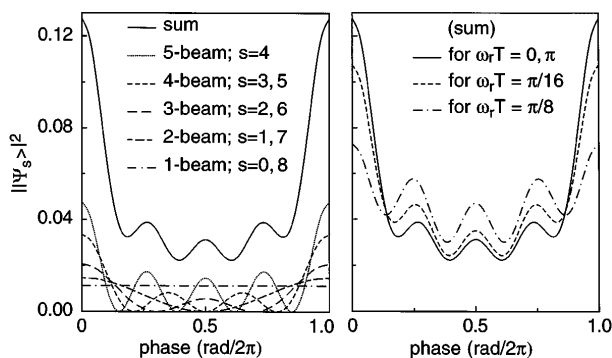

FIG. 2. Left: Calculated total interference signal (solid) of an atomic multiple beam interferometer and contributions to this signal from the different families of interfering wave packets for small interaction times T ($\omega_r T \rightarrow 0$); also for $\omega_r T = \pi, 2\pi, \ldots$. The fraction of atoms $||\Psi_s\rangle|^2$ remaining in the dark state after the pulses is shown as a function of the phase of the third pulse. Right: Calculated total interference signals for different interaction times T.
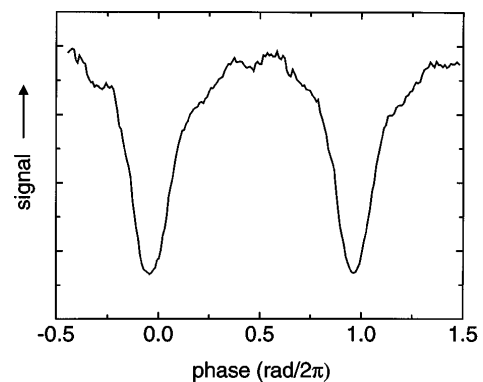

FIG. 3. Ramsey fringes observed with copropagating laser beams for a sequence of two pumping pulses. The graph gives the fluorescence lock-in signal (0.1 s integration time/point) detected during the second pulse as a function of the phase of the second laser pulse.
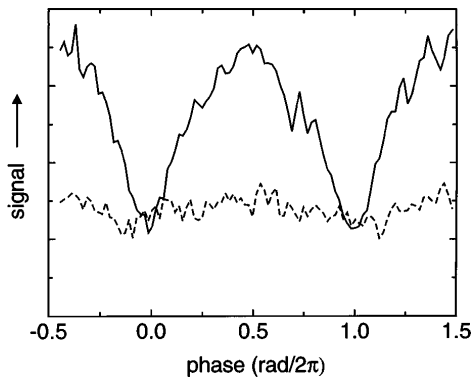
FIG. 4. Experimental interference signals (solid) of an atomic multiple beam interferometer with three pulses and counterpropagating beams, as shown in Fig. 1. The fluorescence lock-in signal (0.1 s integration time/point) detected during the third pulse is shown as a function of the phase of this pulse. For comparison, the dashed line shows the signal detected during the second pulse as a function of the phase of the second pulse. Since the interferometer paths here still are largely separated, almost no interference signal is observed.

Once the Ramsey signals were understood, we moved to an atomic interferometer sequence with three resonant pulses as shown in Fig. 1(b), now using counterpropagating optical beams. For the first pumping pulse we started with a 1.3 μs long period of low intensity to select a velocity slice Δv_z of $2k\Delta v_z/2\pi \approx 200$ kHz Doppler width from our initial Doppler distribution of 1.2 MHz (we give here the widths for a two-photon transition) [13]. The lower intensity gives a smaller velocity width of the dark state. Velocity selection is mandatory, because otherwise the frequency width of the optical pulses (≈ 600 kHz) is not significantly above the Doppler width of the atoms. The intensity is then increased to full value for 0.7 μs. This pulse length is also used for the next two pulses. The selected atomic velocity width corresponds to an atomic wave packet size of roughly $\hbar/2m\Delta v_z \approx 17$ nm, whereas the spatial separation between two adjacent interferometer arms is $2\hbar kT/m = T(6.67$ mm/s) after a drift time T.

Typical interferometer signals are shown in Fig. 4 (solid line) for a time $T = 5$ μs between the pulses, where the phase of the third pulse was varied. The plot shows the fluorescence emitted during the third pulse which recombines the atomic partial waves. The experimental width of the dip is $0.32 \times 2\pi$, which is clearly broader than the expected value of $0.18 \times 2\pi$. We believe that the larger width of the Doppler-sensitive interferometer signal is mainly due to the large initial atomic velocity spread parallel to the laser beams. Nevertheless, the observed widths of the principal maxima are still considerably below the value $0.5 \times 2\pi$ observed in conventional two-beam interferometer experiments.

For future improvements of the experimental setup, the use of laser-cooled atoms in an atomic fountain should allow considerably longer interaction times between the pulses of up to $T = 200$ ms. The atom should be launched into a magnetic shield [7], which suppresses stray magnetic fields. The use of laser-cooled cesium atoms with a temperature of a few μK would allow one to omit the velocity preselection, when similar optical beam intensities as in the present setup are used.

One may also think of interferometers with a higher number of interfering paths using some isotopes of heavy atoms, or molecules with a high rotational quantum number and a very large number of m_F sublevels. Alternatively, multiple beam interferometers could be realized by recombining the diffraction pattern of an atom from an off-resonant focused standing wave [14]. Here, however, the occurring ac Stark shift will introduce systematic phase shifts.

[1] See, for example, articles in Appl. Phys. B **54**, 321ff (1992).

[2] M. Kasevich and S. Chu, Phys. Rev. Lett. **67**, 181 (1991).

[3] D. S. Weiss, B. C. Young, and S. Chu, Phys. Rev. Lett. **70**, 2706 (1993).

[4] See, for example, E. Hecht and A. Zajac, *Optics* (Addison-Wesley, Reading, MA, 1974).

[5] P. Marte, P. Zoller, and J. L. Hall, Phys. Rev. A **44**, R4118 (1991).

[6] J. Lawall and M. Prentiss, Phys. Rev. Lett. **72**, 993 (1994); L. C. Goldner *et al.,* Phys. Rev. Lett. **72**, 997 (1994).

[7] M. Weitz, B. C. Young, and S. Chu, Phys. Rev. Lett. **73**, 2563 (1994).

[8] C. J. Bordé, Phys. Lett. A **140**, 10 (1989).

[9] E. L. Hahn, Phys. Rev. **80**, 580 (1950).

[10] C. J. Foot, H. Wu, E. Arimondo, and G. Morigi, J. Phys. II (France) **4**, 1913 (1994), and references therein.

[11] C. Cohen-Tannoudji, in *Les Houches 1990, Session LIII,* edited by J. Dalibard, J.-M. Raimond, and J. Zinn-Justin (North-Holland, Amsterdam, 1992).

[12] J. Schmiedmayer *et al.,* J. Phys. II (France) **4**, 2029 (1994).

[13] This selection mechanism is related to the work on velocity selective coherent population trapping in subrecoil laser cooling, where a closed atomic transition is used [11]. We apply pumping pulses tuned to an open atomic transition, so that atoms that are not in the velocity dependent dark state and coupled to the light will mostly be pumped into the $F = 3$ hyperfine state and not detected. This is essential at least for the later interferometer pulses to preserve coherence.

[14] B. Ya. Dubetskii, A. P. Kazantsev, V. P. Chebotaev, and V. P. Yakovlev, JETP Lett. **39**, 649 (1984).